Journal of Materials Science: Materials in Electronics (2019) 30:8876–8882
https://doi.org/10.1007/s10854-019-01215-1

Investigation of physical properties and surface free energy of produced ITO thin films by TVA technique

Saliha Elmas[1] · Şadan Korkmaz[1] · Suat Pat[1]

Received: 22 November 2018 / Accepted: 25 March 2019 / Published online: 2 April 2019

Abstract

In this study, tin-doped indium oxide (ITO) thin films with composition of 10% SnO_2 and 90% In_2O_3 have been produced onto glass, polyethylene terephthalate (PET) and Silicon (Si) substrates by using thermionic vacuum arc technique. The properties of the ITO thin films were determined various tolls such as an X-ray diffraction (XRD), ultraviolet–visible (UV–Vis) spectrophotometer, optical reflectometer, field emission electron microscopy (FESEM), atomic force microscopy, four-point probe and contact angle (CA) measurements devices. According to the XRD patterns, deposited thin films onto glass, PET and Si substrate are in amorphous structure. The thicknesses of the deposited layers are very close to each other's and films. The transmittance values are approximately 30% at 632 nm. Refractive index of the deposited layers are close to 1.75, but optical band gaps are found 3.88 and 3.81 eV for the thin film deposited onto glass and PET substrate, respectively. These values are bigger than the value of the band gap value of the ITO material. In surface analysis, it was found that crystallite dimensions are in nano-scales. According to surface analysis, nano-crystalline ITO thin films were deposited. The contact angle of the coated ITO layer were measured in the range of 98°–110°. The electrical resistivity of films was calculated about 0.65×10^{-5} Ω cm for ITO/glass, 1.05×10^{-5} Ω cm for ITO/PET and 5.82×10^{-5} Ω cm for ITO/Si.

1 Introduction

Transparent conductive oxide (TCOs) materials have been studied still extensively in recent years due to their optical transparency and high electrical conductivity. Tin doped indium oxide (ITO) is indispensable material among all TCOs and today this material is utilized in numerous systems such as electronics and semiconductor industries [1, 2]. ITO is known that n-type degenerate semiconductor and has relatively wide energy gap of 3.5–4.3 eV [3]. ITO stands out not only for its excellent electrical properties (low sheet resistance ~ 10 Ω/sq.), but also due to its high optical transmittance (> 90%) in the visible range of the spectrum and has high IR reflectance at longer wavelengths [4–6]. Electrical, morphological and optical properties of ITO thin films strongly depend on the experimental method. There are many techniques have been used to grow ITO thin film on glass and different polymers, such as polyethylene naphthalate (PEN), polyaniline (PANI), polyethylene terephthalate (PET) and etc. The deposition techniques change the on electrical and optical properties of the deposited thin film [1, 7]. The oxygen partial pressure, substrate temperature, rate of deposition, deposition technique, nature of substrate and post-treatment parameters are critical parameters produced by vacuum techniques [8, 9]. Deposition of ITO thin films on glass or on flexible polymer substrates is used numerous methods, such as ion assisted plasma evaporation [10], electron beam evaporation [11, 12], radio frequency (RF) magnetron sputtering [13–16], pulsed laser deposition (PLD) [17, 18], spray pyrolysis [19], sol–gel process [20], chemical vapour deposition [21] and etc. ITO thin films have been used in many technological applications of optoelectronic devices such as touch panels [22], photovoltaic cells [23], organic light-emitting devices (OLED) [24], transparent thin films transistors [25], light emitting diodes (LED) [26], antireflection coatings, and gas sensors [27] and liquid crystal display (LCD) [28], and etc.

In this paper, the structural, optical, electrical, morphological properties and surface free energy of ITO thin films deposited by thermionic vacuum arc (TVA) technique were investigated. Polyethylene terephthalate (PET) is a popular non-conducting polymer material because of transparent, cheaper, good gas barrier and easy manufacturability

✉ Suat Pat
suatpat@ogu.edu.tr

[1] Department of Physics, Eskisehir Osmangazi University, 26480 Eskisehir, Turkey

[29]. Also, glass, PET and silicon (Si) substrates were used for the comparison. The crystal structures of the produced ITO thin films were analysed by X-ray diffraction (XRD) analysis. The surface properties of the ITO thin films were characterized by field emission scanning electron microscopy (FESEM) and an atomic force microscopy (AFM) system. Thickness, reflection and refractive index values were measured. Transmittance spectrum was determined with a Unico UV–Vis spectrophotometer and electrical resistivity of the ITO thin films was studied four-point probe method at room temperature. The Wettability of the material have been measured by contact angle (CA) analysis methods. In particular, we have focused on investigate the wettability of the ITO layers by means of contact angle (CA) measurements.

2 Experimental details

TVA is an anodic plasma generator and it does not use a buffer gas such as argon, neon, etc. This is the fundamental difference from plasma-assisted technologies. The TVA is also thin film growth technique. TVA creates pure material plasma. In our study, ITO pellets as anode material in tungsten crucible have been used [30–41]. A highly pure (99.999%) indium tin oxide (ITO) is a solid solution of indium oxide (In_2O_3) and tin oxide (SnO_2), with typically 90% wt In_2O_3, 10% wt SnO_2. TVA technique was used for the ITO thin films deposition on glass, PET and Si substrates. TVA discharge occurring between cathode and anode under high or ultra vacuum conditions. An electron gun as a cathode was used to evaporation of the material. As an anode, tungsten evaporation boat was used. The distance between anode and cathode was kept constant as to be 5–6 mm. ITO pellets were placed into tungsten evaporation boat. In the deposition process, the vacuum chamber was pumped down to base pressure (9×10^{-5} torr). After we generate materials plasma in a vacuum chamber by high voltage. During the deposition of ITO thin films by the TVA technique, vacuum chamber pressure was 6.5×10^{-5} torr. Filament current applied to cathode was 21 A and voltage applied to the space between anode and cathode was 400 V. The discharge current created between anode and cathode was 1.8 A. The deposition process was carried out in just 7 min at room temperature. However, produced of ITO thin films have high quality, high purity, low roughness, high adhesion homogeneities and hydrophobic.

3 Results and discussion

X-ray diffractometer (XRD) (Rigaku-rint-2200) with Cu–K_α radiation between $20° \leq 2\theta \leq 70°$ was used for phase analysis and determining the structural properties of ITO thin films. Figure 1 and Table 1 show the XRD spectra of the ITO thin films deposited onto different substrates. It can be seen that deposited ITO thin films are in amorphous form. In Fig. 1, there is no diffraction peak of ITO thin film. However, observed low-intensity peaks of ITO thin film on PET at the different 2θ values come from the PET substrate. (222) is a ITO crystalline peak, Crystallite layers must have the (222) peak or another.

The optical properties of ITO thin films strongly depend on band structure; impurity levels, processing technique, microstructure and etc. The optical transmittance was investigated in the wavelength range of 300–1000 nm by using UNICO UV–Vis double beam spectrophotometer. Figure 2 shows the transmittance spectra of ITO thin films deposited onto different substrates and obtained values were listed in Table 1. In Fig. 2, transparencies of ITO thin films are low at short wavelengths and average transmittance of about 30% at wavelength of 632 nm. As seen in Fig. 2, not only transmittance of ITO/glass but also transmittance of ITO/PET are lower than un-coted substrates. In this case, produced ITO thin films behaved as an opaque material. This situation is related to the energy of the incident light. If the photon's energy is smaller than the band gap of ITO thin film, electrons in the valence band cannot be excited and cannot pass into the conduction band. Grain boundary in the ITO thin film absorbs the visible light and exhibits high absorbing properties. Transmittance values of ITO thin films increases continuously as the wavelength increases. Also, transmittance of produced ITO/glass thin film is lower than ITO/PET thin film in visible region. This situation indicated that not only opaqueness but also oxygen vacancies, surface roughness and effect of substrate [42]. However, it is well known that the transmittance of films depends upon the crystallinity of the films. According to XRD results, ITO thin films are exhibited amorphous form.

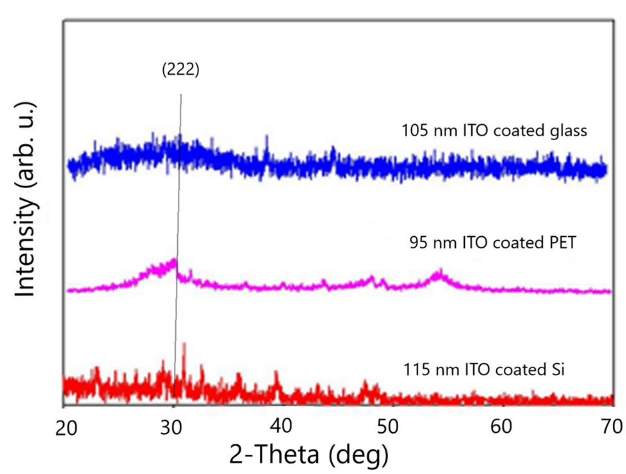

Fig. 1 XRD patterns of ITO thin films

Table 1 Structural, optical and morphological properties of ITO thin films deposited onto the substrates by TVA technique

Sample	Crystal system	Thickness (nm)	Average optical transmittance (%)	Refractive index (n)	Optical band gap (eV)	Porosity	RMS surface roughness (nm)
ITO/glass	Amorphous	105	28	1.99	3.88	13.19	0.93
ITO/PET	Amorphous	95	30	1.96	3.81	5.28	2.40
ITO/Si	Amorphous	115	–	–	–	–	1.41

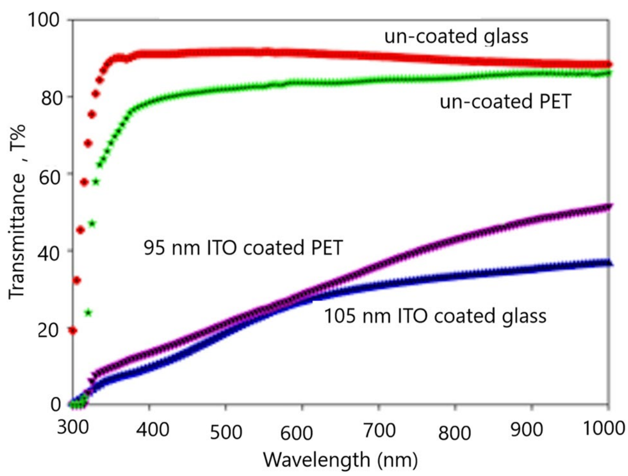

Fig. 2 Transmittance spectra of ITO thin films

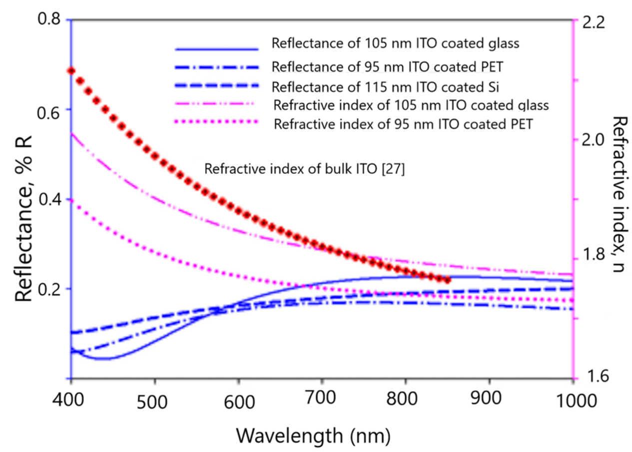

Fig. 3 Refractive index and Reflectance of ITO thin films

Thickness, refractive index and reflectance spectra of the prepared samples are measured by using Filmetrics F20 thin film analyser device. A Filmetrics F20 thickness measurement system was used for reflection measurements. Filmetrics measures a film's thickness by reflecting light of the film and analysing the reflected light over different wavelengths. This technique is called spectral reflectance, and it has considerable advantages in speed, simplicity, and cost, especially over common techniques such as ellipsometer and profilometry. Average thicknesses of ITO thin films were determined 105 nm ITO/glass, 95 nm ITO/PET and 115 nm ITO/Si by means of Filmetrics F20 tools (Table 1).

Figure 3 shows the variations of refractive index and reflectance of ITO thin films in UV–Vis–NIR region. It can be concluded that prepared ITO thin films on PET and Si substrates exhibit similar reflectivity in the visible region and ITO thin film on glass exhibits higher reflectivity than the others. Also, Fig. 3 shows that while refractive index of the ITO thin films decreases with increasing wavelength in the optical region. It should be noted that the refractive index values are ranging from 1.96 to 1.99 in the UV–NIR region for ITO/PET and ITO/glass at 550 nm (Table 1). Refractive index of bulk ITO has been taken from Ref. [43]. Measured refractive index of ITO thin films are in agreement with literature [44].

The porosity of ITO thin films was calculated using the expression given below:

$$\text{Porosity} = \left(1 - \frac{n^2 - 1}{n_d^2 - 1}\right) \times 100\,(\%), \quad (1)$$

where n_d is the refractive index of pore-free ITO is 2.1 and n is the refractive index of the porous thin films [44]. The calculated porosity of films were listed in Table 1.

The important optical parameter is the band gap of materials. Band gap of a semiconductor gives information about its electrical and optical properties. The optical band gap (E_g) values calculated from the plot of $(\alpha h\nu)^2$ versus $\alpha h\nu$, where α is the absorption coefficient. Band gap of the ITO thin films are defined by using their absorbance data. Figure 4 shows the band gap graphs of the deposited layer. It is well known that the fundamental band gap of ITO films is greater than 3.7 eV and varies in a wide range from 3.7 to 4.5 eV [44]. It is calculated that E_g values are from 3.88 to 3.81 eV for ITO/glass and ITO/PET respectively (Table 1). According to Fig. 4, calculated E_g values are very close to related literature values [45]. It can be seen that the ITO/PET has a lower band gap value than ITO/glass. This difference is approximately 70 meV. This

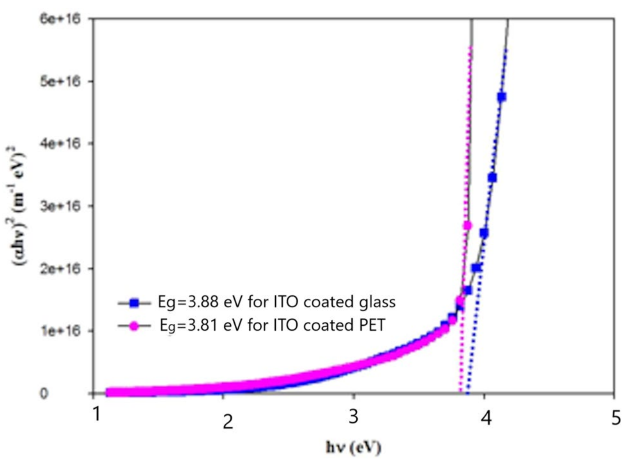

Fig. 4 Dependence $(\alpha h\nu)^2$ versus hν for ITO thin films

decrease may be related to crystalline properties, grain distribution differences or substrate effect.

AFM is commonly used to characterization of surface topography. Surface morphologies and surface roughness of the ITO thin films were analysed on AFM (Ambios Q-scope Atomic Force Microscope) by non-contact mode using the Scan Atomic V 5.1.0 SPM control software at room temperature and the scan area was (4×4) µm^2. Root mean square (RMS) roughness values were obtained by AFM software and measured values shown in Table 1. The AFM and FESEM images of ITO thin films are shown in Fig. 5. As seen in Fig. 5, there is no obvious formation and the surfaces are completely amorphous and the roughnesses are quite lower. Also AFM and FESEM images of films show that ITO thin films are smoother, clear granular, uniform and densely formed surface profile. The AFM images are in a good accordance with the XRD data discussed in Fig. 1. However, as seen in FESEM images, grain sizes of ITO thin films are determined in range of 22–40 nm. The roughnesses of deposited ITO thin films are very low and these values are in agreement with TVA literature [30–41]. The uncoated PET substrate has high surface roughness of approximately 3 nm. ITO/PET thin film has high roughness among prepared ITO thin films. We can see that affect of substrates in the ITO coated films.

Measuring the contact angle is a useful technique to determine the free energy of a surface [46–49]. Superhydrophobic surfaces (high water contact angle (CA) $\theta_c > 150°$) exhibit unique characteristics and are used for applications such as solar panels, optical devices and self-cleaning windows. In order for a surface to exhibit superhydrophobic properties, rough of surface must have [50]. Various surface treatments on ITO thin films were investigated by Vacca et al. [51]. They reported that both surface roughness and surface energy are the most important parameters. In our study, we want to investigate the wettability of produced ITO thin films on different substrates by TVA technique. Wettability properties of ITO thin films were determined by measuring their contact angle (θ). The contact angle value was strongly dependent on the liquid used. To obtain contact angle values for ITO thin films were used water because of a polar molecule with a large dipole moment. This property of water leads to achieve high surface tension. Optical tensiometer (Attension Theta Lite) was used for evaluating wetting behaviour of the water for the ITO thin films surfaces. The equation of state approach is mathematically calculate the surface free energy (SFE) of solids and this approach requires the measurement to be done only by using one liquid. It is know that properties of spreading liquid on substrate present film quality. In our experiments, the contact angles were found and the surface free energy values were calculated with Equation of State approach. Obtained measurement results were summarized in Table 2. These results show that produced ITO thin films exhibited hydrophobic behaviour and indicate that the water was wetting the ITO thin films surface weakly.

The sheet resistance R_s and the film electrical resistivity measurements are performed using a four-point probe by using Jandel Model RM3-AR device at room temperature and the effects of different substrates on the electrical resistivity of ITO thin films are investigated. The correlation between sheet resistance and electrical resistivity can be defined with the following equation [8]:

$$\rho = R_s x d \tag{2}$$

where R_s is the sheet resistance of thin film, ρ is the electrical resistivity and d is the thickness.

Resistivity and sheet resistance of produced ITO thin films were measured. The obtained values for the ITO thin films on different substrates were listed in Table 3.

Produced ITO/PET thin film has the lowest sheet resistance value among others. The sheet resistance studies shows that the sheet resistance value of ITO thin films produced by TVA technique depend on substrates. According to literature studies suggested that effect of particle size and grain boundary scattering significant factor affecting the electrical properties of ITO thin films. So, in this study, decreasing of electrical resistivity of the ITO films may be due to the surface properties became effective.

4 Conclusion

In summary, ITO thin films with composition of 10 wt% SnO_2 and 90 wt% In_2O_3 have been produced by TVA technique and substrate is an important factor to determine some physical properties of ITO thin films. ITO thin films with various thicknesses have characterized as well in order to be

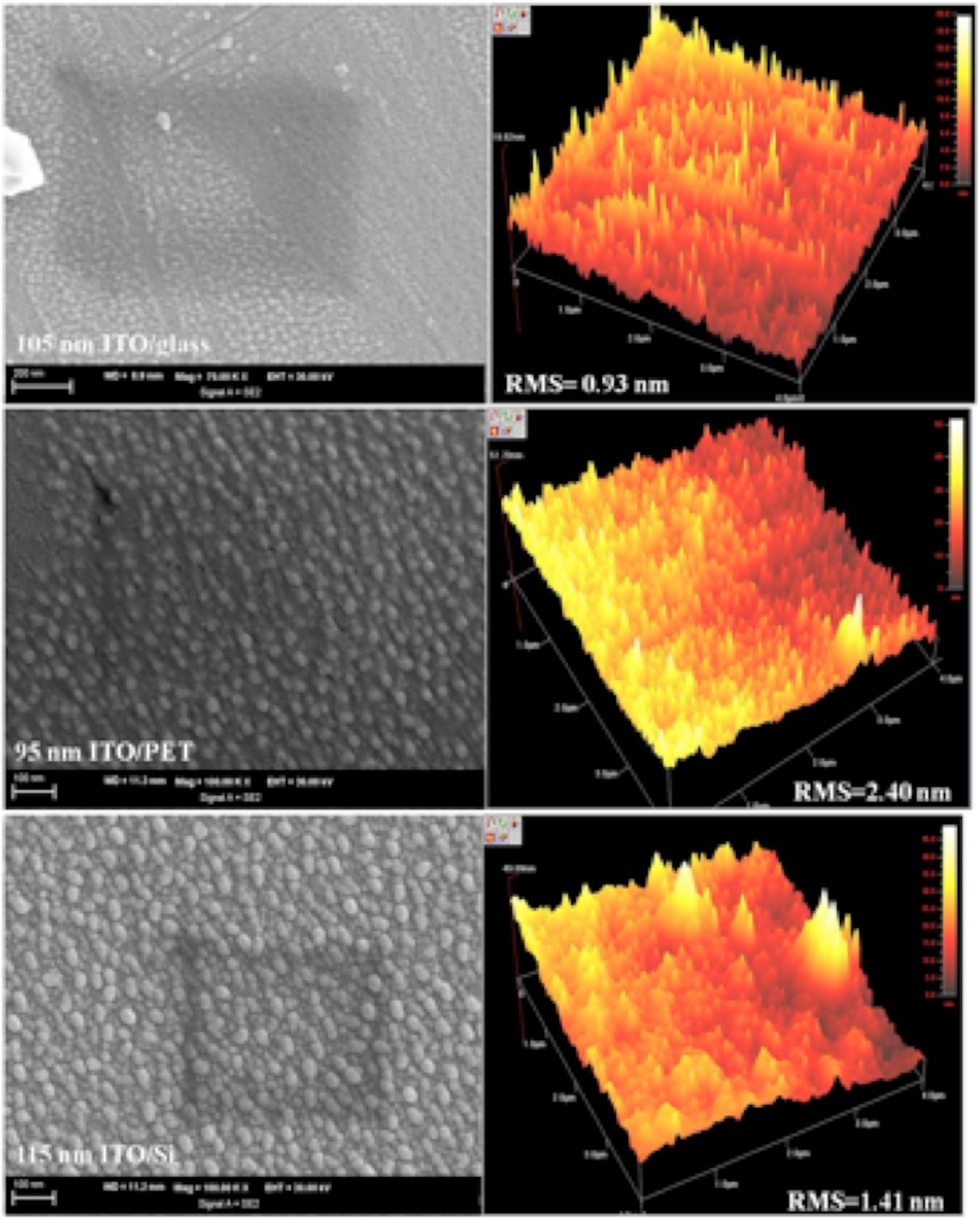

Fig. 5 FESEM and AFM images of ITO thin films

Table 2 CA and SFE values of ITO thin films

Sample code	Heavy media	CA (°)	Method	SFE γ (mN/m)
ITO/glass	Water	104	Equation of state	20
ITO/PET	Water	110		16
ITO/Si	Water	98		24

able to make a comparison different substrates. If ITO thin films are deposited on an untreated substrate, the associated organic solar cell usually exhibits poor performance. So the surface of the ITO thin films are treated various surface treatments for enhancement efficiency over the untreated organic solar cell and the surface properties of the ITO thin films strongly depend on the treatment methods. The surface

Table 3 The measured electrical parameters of the deposited ITO thin films

Samples	Resistivity (Ω cm) × 10^{-5}	Sheet resistance (Ω/☐)
ITO/glass	0.65	4.09
ITO/PET	1.05	2.44
ITO/Si	5.82	23.34

energy of thin films for optoelectronic applications plays an important role. We have investigated the wettability of the ITO thin films by means of contact angle measurements. The measurements of contact angles show that produced ITO thin films have exhibited hydrophobic behaviour. The structural and morphological studies have discussed and the structures of all prepared ITO thin films have found amorphous form and surface roughnesses have had drastically low. However AFM and FESEM images showed a grainy structure. Optical properties of ITO thin films were studied in the UV–Vis–NIR region and transmission values were decreasing with increasing thickness as well as band gap of the films were found. Moreover, ITO thin films were calculated porosity and ITO/glass porosity was higher than ITO/PET. Produced ITO/PET thin film has the lowest sheet resistance value among others.

References

1. K.S. Tseng, Y.L. Lo, Appl. Surf. Sci. **285P**, 157–166 (2013)
2. S.D. Senol, A. Senol, O. Ozturk, M. Erdem, J. Mater. Sci.: Mater. Electron. **25**, 4992–4999 (2014)
3. A. Kosarian, M. Shakiba, E. Farshidi, J. Mater. Sci.: Mater. Electron. **28**, 787–797 (2017)
4. K.P. Sibin, G. Srinivas, H.D. Shashikala, A. Dey, N. Sridhara, A.K. Sharma, H.C. Barshilia, Sol. Energy Mater. Sol. Cells **172**, 277–284 (2017)
5. C. McDonnell, D. Milne, C. Prieto, H. Chan, D. Rostohar, G.M. O'Connor, Appl. Surf. Sci. **359**, 567–575 (2015)
6. A.P. Amalathas, M.M. Alkaisi, J. Mater. Sci.: Mater. Electron. **27**, 11064–11071 (2016)
7. A. Bera, K. Deb, V. Kathirvel, T. Bera, R. Thapa, B. Saha, Appl. Surf. Sci. **418**, 264–269 (2017)
8. L. Hao, X. Diao, H. Xu, B. Gu, T. Wang, Appl. Surf. Sci. **254**, 3504–3508 (2008)
9. E. Celik, U. Aybarc, M.F. Ebeoglugil, I. Birlik, O. Culha, J. Sol-Gel. Sci. Technol. **50**, 337–347 (2009)
10. K. Füchsel, U. Schulz, N. Kaiser, A. Tünnermann, Appl. Opt. **47**, C297–C302 (2008)
11. D.C. Paine, T. Whitson, D. Janiac, R. Beresford, C.O. Yang, B. Lewis, J. Appl. Phys. **85**, 8445–8450 (1999)
12. M. Quaas, C. Eggs, M.L. Ma, H. Wulff, Thin Solid Films **322**, 277 (1998)
13. V. Sittinger, F. Ruske, W. Werner, C. Jacobs, B. Szyszka, D.J. Christie, Thin Solid Films **516**, 5847–5859 (2008)
14. S. Ray, R. Banerjee, N. Basu, A.K. Batabyal, A.K. Barua, J. Appl. Phys. **54**, 3497 (1983)
15. Y. Hu, X. Diao, C. Wang, W. Hao, T. Wang, Vacuum **75**, 183 (2004)
16. M. Gulen, G. Yildirim, S. Bal, A. Varilci, I. Belenli, M. Oz, J. Mater. Sci.: Mater. Electron. **24**, 467 (2013)
17. T.K. Yong, T.Y. Tou, R.B. Yang, B.S. Teo, H.K. Yow, Vacuum **82**, 1445–1448 (2008)
18. J.P. Zheng, H.S. Kwok, Appl. Phys. Lett. **63**, 1 (1993)
19. S. Major, K.L. Chopra, Sol. Energy Mater. **17**, 319 (1988)
20. Y. Djaoued, V.H. Phong, S. Badilescu, P.V. Ashrit, F.E. Girouard, V.V. Truong, Thin Solid Films **293**, 108 (1997)
21. J. Vetrone, Y.W. Chung, J. Vac. Sci. Technol. **A9**, 3041 (1991)
22. S.F. Tseng, W.T. Hsiao, K.C. Huang, D. Chiang, M.F. Chen, C.P. Chou, Appl. Surf. Sci. **257**, 1487–1494 (2010)
23. M. Aleksandrova, N. Kurtev, V. Videkov, S. Tzanova, S. Schintke, Microelectron. Eng. **145**, 112–116 (2015)
24. Y.S. Tsai, F.S. Juang, T.H. Yang, M.C. Yokoyama, L.W. Ji, Y.K. Su, J. Phys. Chem. Solids **69**, 764–768 (2008)
25. G.J. Exarhos, X.D. Zhou, Thin Solid Films **515**, 7025–7052 (2007)
26. Y.H. Tak, K.B. Kim, H.G. Park, K.H. Lee, J.R. Lee, Thin Solid Films **411**, 12–16 (2002)
27. H. Hartnagel, A.L. Dawar, A.K. Jain, C. Jagadish, *Semiconducting Transparent Thin Films* (Institute of Physics, Bristol, 1995), p. 181
28. M. Gaillet, L. Yan, E. Teboul, Thin Solid Films **516**, 170–174 (2007)
29. K. Iiyama, T. Ishida, Y. Ono, T. Maruyama, T. Yamagishi, IEEE Photon. Technol. Lett. **23**, 275–277 (2011)
30. S. Pat, N. Ekem, T. Akan, Ö. Küsmüs, S. Demirkol, R. Vladoiu, C.P. Lungu, G. Musa, J. Optoelectron. Adv. Mater. **7**, 2495–2499 (2005)
31. V. Şenay, S. Özen, S. Pat, Ş. Korkmaz, J. Alloys Compd. **663**, 829–833 (2016)
32. S. Elmas, S. Korkmaz, S. Pat, Appl. Surf. Sci. **276**, 641–645 (2013)
33. R. Mohammadigharehbagh, S. Özen, H.H. Yudar, S. Pat, Ş. Korkmaz, J. Mater. Sci.: Mater. Electron. **28**, 14131–14137 (2017)
34. E. Şilik, S. Pat, S. Özen, R. Mohammadigharehbagh, H.H. Yudar, C. Musaoğlu, Ş. Korkmaz, Thin Solid Films **640**, 27–32 (2017)
35. S. Özen, S. Pat, H.H. Yudar, Ş. Korkmaz, Z. Pat, Vacuum **153**, 112–116 (2018)
36. M.Z. Balbag, S. Pat, M. Ozkan, N. Ekem, G. Musa, Phys. B Condens. Matter **405**, 3276–3278 (2010)
37. S. Pat, S. Özen, Ş. Korkmaz, J. Electron. Mater. **47**, 167–172 (2018)
38. S. Özen, S. Pat, V. Şenay, Ş. Korkmaz, Vacuum **135**, 50–54 (2017)
39. S. Elmas, S. Pat, R. Mohammadigharehbagh, C. Musaoğlu, M. Özgür, U. Demirkol, S. Özen, Ş. Korkmaz, Phys. B **557**, 27–33 (2019)
40. U. Demirkol, S. Pat, R. Mohammadigharehbagh, C. Musaoğlu, M. Özgür, S. Elmas, S. Özen, Ş. Korkmaz, J. Mater. Sci.: Mater. Electr. **29**, 18098–18104 (2018)
41. M. Ozgür, S. Pat, R. Mohammadigharehbagh, C. Musaoglu, U. Demirkol, S. Elmas, S. Ozen, S. Korkmaz, J. Alloys Compd. **2019**(774), 1017–1023 (2018)
42. S.H. Mohamed, F.M. El-Hossary, G.A. Gamal, M.M. Kahlid, Acta Phys. Pol., A **115**, 704–708 (2009)
43. Refractive index database. http://refractiveindex.info/. Accessed 1 August 2018
44. V. Senthilkumar, P. Vickraman, M. Jayachandran, C. Sanjeeviraj, Vacuum **84**, 864–869 (2010)
45. H.R. Fallah, M.G. Varnamkhasti, M.J. Vahid, Renew. Energy **35**, 1527–1530 (2010)
46. H.R. Fallah, M. Ghasemi, A. Hassanzadeh, H. Steki, Phys. B **373**, 274–279 (2006)

47. Y.T. Cheng, J.J. Ho, C.K. Wang, W. Lee, CCh. Lu, B.S. Yau, J.L. Nain, S.H. Chang, C.C. Chang, K.L. Wang, Appl. Surf. Sci. **256**, 7606–7611 (2010)
48. Z.Z. You, J.Y. Dong, Appl. Surf. Sci. **253**, 2102–2107 (2006)
49. Z.Z. You, Mater. Lett. **61**, 3809–3814 (2007)
50. D. Ebert, B. Bhushan, Langmuir **28**, 11391–11399 (2012)
51. P. Vacca, M. Petrosino, A. Guerra, R. Chierchia, C. Minarini, D.D. Sala, A. Rubino, J. Phys. Chem. C **111**, 17404–17408 (2007)